Indian Journal of Pure & Applied Physics
Vol. 63, September 2025, pp. 823-830
DOI: 10.56042/ijpap.v63i9.19825

# Investigations on Structural, Optical, Mechanical, Thermal and Biological Properties of Pure and Crystal Violet Dye Doped L-Asparagine Single Crystals

P Shiny Christina[a], D Jencylin Navarani[a,*]& S C Vella Durai[b]

[a]Department of Physics and Research Centre, Sarah Tucker College,Tirunelveli 627 007, India

[b]PG and Research Department of Physics, Sri Paramakalyani College, Tenkasi 627 412, India

*Received: 18th May 2025; accepted: 10th July 2025*

An organic material, L-asparagine monohydrate (LAM) is doped with crystal violet dye to enhance the host crystal's various characteristics. Slow evaporation has been used to create both pure and Crystal Violet-doped L-asparagine crystals.After 15 days, Pure L-asparagine crystals were produced and after 25 days, Crystal violet doped L-asparagine crystals were produced. Single crystal XRD evaluation has been used to determine the crystal system and unit cell dimensions. Pure L-Asparagine crystal was found to have orthorhombic crystal structure and CV doped LAM was found to have triclinic crystal structure. Using Powder XRD analysis, prominent peaks observed in the xrd pattern have been indexed in order to characterize its structure by evaluating the miller indices (hkl) values. UV-Vis Analysis has been done between 200 and 800 nm wavelength range. The band gap energy value for pure sample was found to be 4.88 eV and doping resulted in a larger energy band gap value as 4.97 eV and an enlarged transmittance window in the transmittance spectra. The pure and Crystal Violet doped LAM samples' linear optical characteristics have been assessed. The mechanical property of the generated crystals was assessed using the Vickers microhardness test. A number of mechanical characteristics of both pure and doped LAM crystals have been assessed, including the stiffness constant, yield strength, brittleness index, and hardness number. The thermal stability of the produced crystal was understood using the thermal analysis technique. Four strains of Pseudomonas aeruginosa, Klebsiella pneumonia, Streptococcus mutans, and Staphylococcus aureus were used to investigate the antibacterial activity using the Agar disk diffusion test. The samples Pure LAM and Crystal Violet doped LAM were found to have the highest activity of 22 mm against Streptococcus mutans. As a result, the produced samples were discovered to have numerous uses in the fields of biomedicine, water purification, and electro-optics.

**Keywords:** Structural, Optical, Mechanical, Thermal, Antibacterial activity, Single Crystal

## 1 Introduction

Several industries, including semiconductor technology, photonics, and optoelectronics, have been greatly impacted in recent decades.[1, 2] It is well known that new metal-based amino acid compounds can be created by the reaction of metal salts and amino acids[3]. Because of its higher non-linear coefficient, rapid electro-optic effect response, and more stable physical and chemical properties, organic materials are gaining popularity. Because of their high electrical sensitivity ($\chi$), which is brought on by molecular hyperpolarisability ($\beta$), organic materials have been demonstrated to be dominant to conventional inorganic substances[4].Asparagine, one of the amino acids, was crystallized and extracted from asparagus juice, which contains a lot of it. Pierre Jean Robinquet found another chemical with properties similar to asparagine a few years later, in 1809. Plisson made another discovery of asparagine in 1828. As a non-essential amino acid, it is not required for food and can be produced by humans from intermediates in the central metabole pathway[5].Crystal violet (CV; tris (p-(dimethylamino)phenyl)methyl) is an organic dye that belongs to the important industrial dye class called triphenylmethane (TPM). CV dye has numerous applications in the medical field as an active ingredient in Gram's stain and antibacterial treatments[6, 7]. Both humans and animals can use this dye as an antiseptic and as a pH indicator[8]. Organic dye-doped crystals might be a good alternative to laser gain media due to their high thermal stability, intrinsic polarization, and reduced scattering[9]. In our knowledge, there is no study on crystal violet (CV) dye doped LAM crystals. The influence of crystal violet dye on the structural, optical, mechanical, thermal and biomedical properties of L-Asparagine Monohydrate single crystals have been investigated.

*Corresponding author: E-mail: jencylin.stc@gmail.com

## 2 Materials and Methods

### 2.1 Materials

The materials used in this single crystal preparation included L-Asparagine Monohydrate, crystal violet dye, and distilled water.

### 2.2 Synthesis and Growth of Crystal Violet Doped L-Asparagine Monohydrate crystals

At first, a homogenous solution of L-asparagine monohydrate was made with a solvent of double-distilled water, by stirring it continuously for 5 hrs. By using high quality filter paper, the solution was filtered and was left undisturbed in a beaker with holes in it so that crystals can form using the slow evaporation method. After durationof about 12 days, high quality crystals were grown. Secondly, commercially available high quality crystal violet dye was purchased. Secondly, L-asparagine monohydrate was made into a saturated solution, to which 1 mole% crystal violet dye was added. A magnetic stirrer was used to continuously swirl the mixture for 5 hrs and was then filtered. The filtered solution was kept in storage and left undisturbed for crystal growth. The nucleation of crystals was seen in the following days and after 20 days good quality CV doped L-Asparagine Monohydrate Crystals were collected. Figure 1 shows images of both pure and Crystal Violet doped LAM crystals.

### 2.3 Characterization Techniques

Single-crystal X-ray diffraction analysis was performed using a D8 Quest diffractometer with MoKα radiation (λ = 0.71073 Å). Powder X-ray diffraction patterns of pure and Crystal Violet dye-doped LAM crystals were obtained using a D8 Advance ECO diffractometer. Optical properties were investigated via UV-Vis spectroscopy using a JASCO V-770 spectrometer. Microhardness measurements were conducted using a Shimadzu HM-200A Vickers tester. Thermal analysis (TG/DTA) was carried out using a LABSYS EVO instrument. Additionally, the crystal's antimicrobial activity was evaluated to explore its potential biological applications.

## 3 Results and Discussion

### 3.1X-ray Diffraction Analysis of a Single Crystal (SCXRD)

The generated crystals were subjected to a single crystal X-ray diffraction examination, L-Asparagine and Crystal Violet dye doped L-Asparagine, and the results were obtained. The obtained data is tabulated below (Table 1). It is clear from the result that the pure LAM crystal has an orthorhombic crystal structure. Whereas the crystal structure changes to Triclinic when it was doped with CV, with only slight modification in the values of the lattice parameters. The slight modification of the crystal system of L-asparagine monohydrate upon doping with crystal violet dye during slow evaporation growth could likely be due to the combination of molecular interaction, steric hindrance, and lattice disruption introduced by the dopant[10]. Figure 2 illustrates the crystal structure of pure LAM crystals and those doped with Crystal Violet (CV) dye.

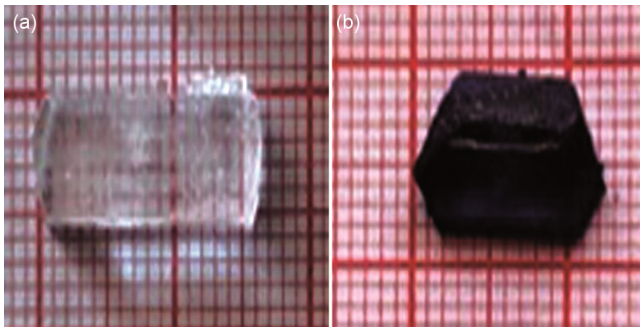


Fig. 1 — (a) Pure LAM (b) CV doped LAM crystal

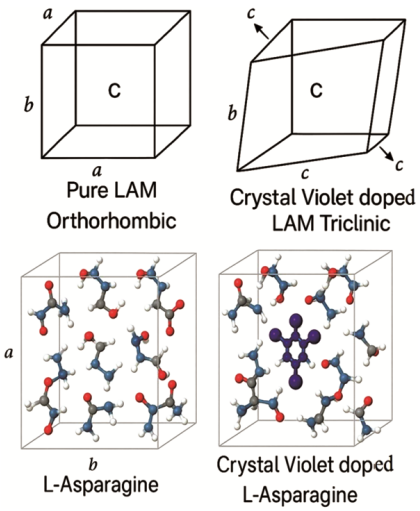


Fig. 2 — Crystal Structure of Pure & CV doped LAM crystals

Table 1 — Unit cell dimensions of Pure and Crystal Violet dye doped LAM crystals

| Parameters | Pure LAM | Crystal Violet doped LAM |
|---|---|---|
| Crystal System | Orthorhombic | Triclinic |
| a (Å) | 5.584 Å | 5.538 Å |
| b (Å) | 9.824 Å | 9.744 Å |
| c (Å) | 11.799 Å | 11.724 Å |
| α (°) | 90° | 89.96° |
| β (°) | 90° | 89.88° |
| γ (°) | 90° | 90.2° |
| Volume, ($Å^3$) | 647.2 $Å^3$ | 632.7 $Å^3$ |

### 3.2 Analysis of Powder X-Ray Diffraction (PXRD)

Analysis of Powder X-Ray diffraction for Pure and Crystal Violet dye doped LAM crystalswas done using the instrument X-ray diffractometer D8 Advance ECO. Powder XRD analysis is the most effective technique for figuring out the grown compound's crystallinity, phase and purity of the sample[11]. To identify the crystal phases using XRD, crushed powder of Pure and Crystal Violet dye doped LAM crystals were examined. The various planes of reflection were indexed using Unit cell software based on the X-ray powder diffraction pattern of the Pure and Crystal Violet dye doped LAM crystals. The obtained pattern of the pure and Crystal Violet doped LAM crystals with indexed reflection peaks are shown in Fig. 3. The pure LAM crystal's XRD pattern is shown by the black line. The peaks show the crystal planes are present in the LAM structure. The CV doped LAM crystal's XRD pattern is displayed by the red line.

The XRD pattern changes when the dopant (CV) is present, signifying the introduction of new phases or modifications to the crystal structure. The extremely high intensity peak at about 20 degrees 2theta, designated (-1 -4 3), seems to be the most notable shift.Thepatterns obtained from the result of pure and Crystal Violet dye doped LAM crystals were analyzed with the help of Unit cell software. The crystal structure experiences lattice strain due to doping with Crystal Violet dye, which causes a minor shift in cell parameter values. It may be inferred that CV doping altered the sample material's space group, crystal system and cell parameter values[12](Table 1).

### 3.3 Optical Evaluation

Numerous optical characteristics, such as localized states, different kinds of optical transitions, and consequently the electronic band structures, are revealed by UV-Vis-NIR studies[13]. For the creation of optical devices, crystals with a broad optical transmittance window and a lower cutoff wavelength in the 200–400 nm regions are preferred[14]. The UV-Visible transmission spectrum of Pure and Crystal Violet doped LAM crystal was recorded between 200-800 nm is shown in Fig. 4.

From the transmission spectrum of the samples, the cut-off wavelengths are observed at 260 nm & 246 nm. Broader absorption peak observed between 520 & 590 nm confirms the existence of Crystal Violet dye[15]. The doping of CV dye results in a 10% improvement in optical transparency and a 16 nm

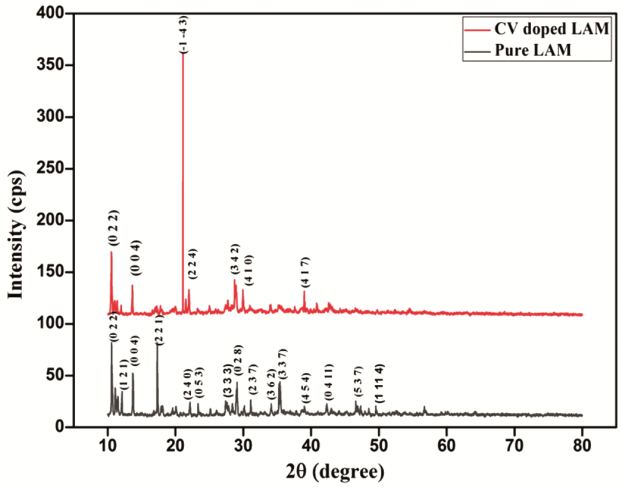


Fig. 3 — Powder XRD patterns of Pure & CV doped LAM crystals

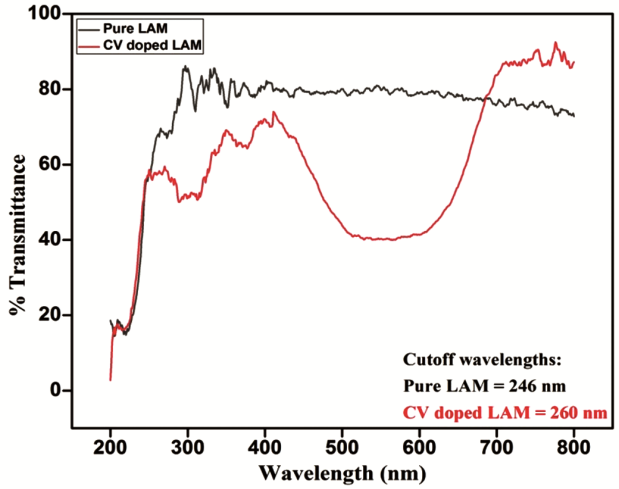


Fig. 4 — Transmission spectra of Pure & CV doped LAM crystals

drop in cutoff wavelength. This crystal shows promise for use in electro-optic applications, since the increase in transparency brought about by CV doping suggests great crystalline perfection [16]. Dye doping causes the cut-off to be lowered, which indicates that these crystals can be used in a variety of optoelectronic applications[17]. Dye-doped crystals can be used as filters because of their considerable absorption in the visible band (450–650 nm) and better transmission in the region (300–450 nm)[18].

The absorption coefficient of the samples can be identified by using the formula,

$$\alpha = \frac{2.303 \times log_{10}(\frac{1}{T})}{d} \quad \ldots (1)$$

where'd'& 'T' indicates the thickness and transmittance of the crystals.Using the relationship

below, which Tauc suggested, the optical band gap was obtained from the transmission spectrum and the absorption coefficient,

$$(\alpha h\nu)^n = A(h\nu - E_g) \quad \ldots (2)$$

Whereas, A= proportionality constant, h= Planck's constant, $E_g$ is the energy band gap value, $\nu$ is the frequency of the incident photon.

A graph (Fig. 5) is drawn for $(\alpha h\nu)^2$ versus $h\nu$, for figuring out the energy band gap. By extending the plot's linear position, energy band gap value can be obtained. Therefore, from the layout of the Tauc, the values obtained for both the samples are 4.88 eV & 4.97 eV respectively.Theoretically, the values are identified by the formula, E=hc/λ (eV), and they were calculated to be 4.7 eV & 5.04 eV for pure and crystal violet dye doped LAM respectively. Generally speaking, materials with band gap energies (>2) larger than two are referred to be insulators or dielectric materials.

The extinction coefficient value for both Pure & CV doped LAM crystal is calculated using the relation given below,

$$k = \frac{\alpha\lambda}{4\pi} \quad \ldots (3)$$

Here, λ is called theincoming photons' wavelength. Figure 6 shows the graph of extinction coefficient versus wavelength. Comparing both Pure & CV doped LAM plot, the extinction coefficient keeps increasing in the visible and NIR region. In CV doped LAM, notably there occurs a broader peak in the visible region verifying that crystal violet dye is present[19].

The linear refractive indices can be evaluated by the use of the formula given below,

$$n = \left(\frac{1}{T} + \left(\frac{1}{T} - 1\right)\right) \quad \ldots (4)$$

T is the transmittance in this case. Figure 7 shows the plot of n vs λ. From the graph, it is clear that the value of refractive index (n) is low for both the crystals. Notably in dye doped crystal the refractive index increases and then decreases (from n=4 to n=1.6). This may be due to high dye concentration. The refractive index of Pure LAM is n=1.4. The elevated values of n along with lower k values for dye doped crystals in comparison to those forpure LAM make them promising and idatesforuseinphotonic device applicationssuchas lightemittingdiodes (LEDs) andimage sensors.

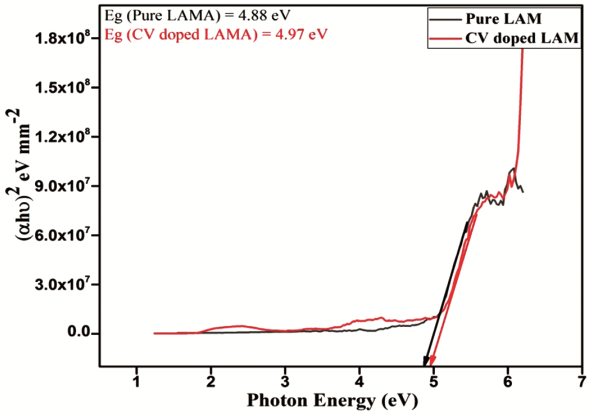


Fig. 5 — Tauc'sPlot of Pure & CV doped LAM crystals

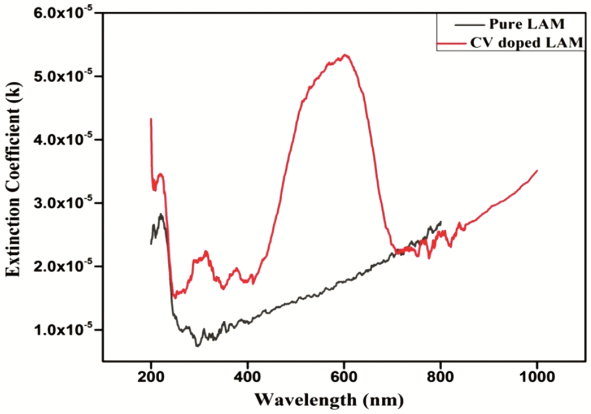


Fig. 6 — Plot of k vs λ of Pure & CV doped LAM crystals

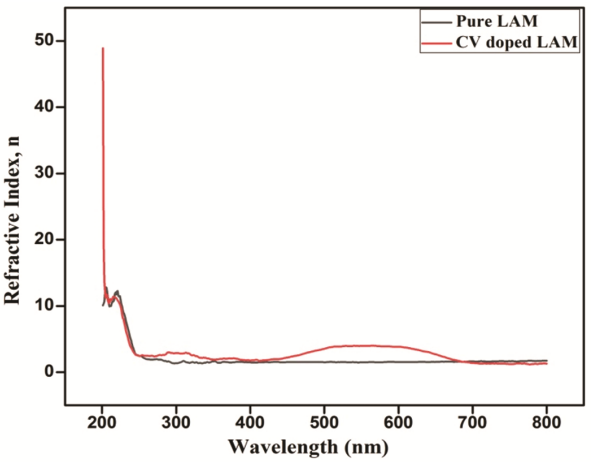


Fig. 7 — Plot of n vs λ of Pure & CV doped LAM crystals

The reflectance of Pure & CV doped LAM crystals can be evaluated from the formula given below [20].

$$R = \frac{(n-1)^2}{(n+1)^2} \quad \ldots (5)$$

Figure 8 shows the reflectance plot of Pure & CV doped LAM crystals. High reflectance is observed in

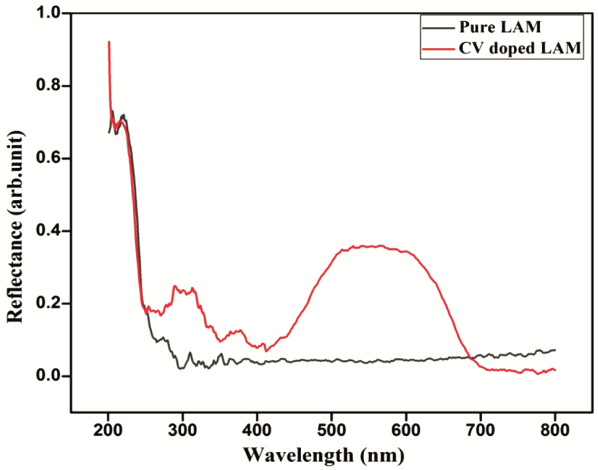


Fig. 8 — Reflectance spectra of Pure & CV doped LAM crystals

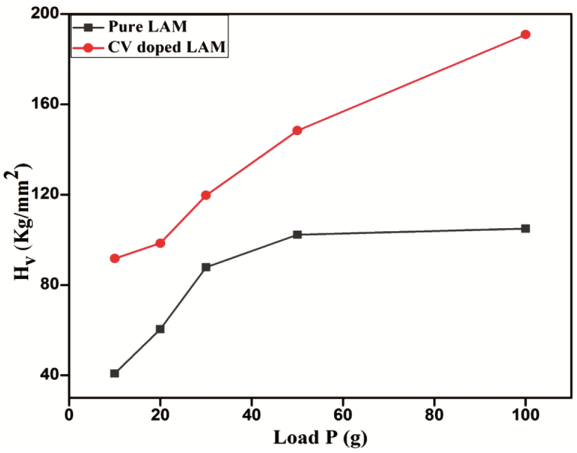


Fig. 9 — Plot of $H_v$vs Load P of Pure CV doped LAM crystals

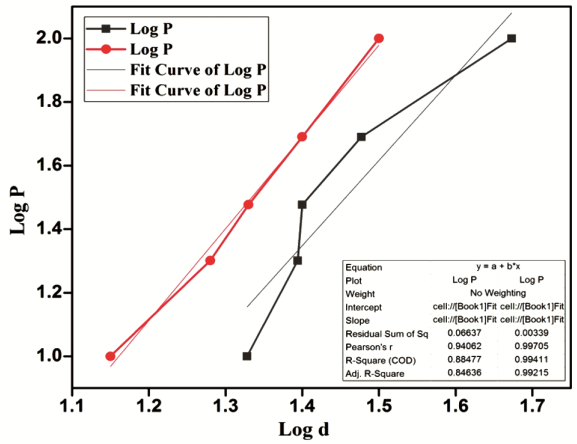


Fig. 10 — Log d vs. Log P plot of Pure CV doped LAM crystals

the cut-off wavelength. The value of reflectance is low for Pure LAM crystal throughout the visible region, whereas for CV doped LAM, a broader peak of higher reflectance is seen throughout the visible spectrum confirming the existence of Crystal Violet dye.

### 3.4. Vickers MicrohardnessTesting

This experiment made use of a pyramidal indenter. The micro hardness number was calculated by measuring the average indentation of the diagonal caused by applying loads. The equation $H_v$= 1.8544 x P / $d^2$, in where d is the length of the indentation diagonally and P is the load applied, was used to determine the $H_v$ values of the Pure and Crystal Violet doped L-Asparagine Monohydrate (LAM) crystals using the average diagonal indentation values. Figure 9 displays the micro hardness against applied load charts for each crystal. For both materials, it is found that the hardness rises as the applied force increases; this is because of the Reverse Indentation Size Effect (RISE)[21].

A sample's capacity to resist penetration by indenters is examined by its hardness number ($H_v$). The existence of fractures, pores, and inclusions has a substantial impact on this, providing crucial information on the formed crystals' tensile and yield strengths. It is observed from the $H_v$ values for Crystal Violet doped LAM crystals are greater than the Pure LAM sample, which may be because of the void space filling property of the material. The nature of the developed crystals was examined by evaluating the crystals' Meyer's index (n). Meyer's law proposes that $P = Ad^n$, where A is a material-specific constant. The values of n, which were derived from the slope of the plot, log d vs. log P are shown in Fig. 10. Meyer's index values were 2.6, 2.8 for the Pure LAM and Crystal Violet doped LAM crystals.

Soft materials have n values greater than 1.6.While for hard materials n lies between 1 and 1.6. Therefore, the synthesized crystals belong to the soft material category.

Using the formula below, the yield strength ($\sigma_y$) can be computed.

$$\sigma_y = \frac{H_v}{2.9}[1-(n-2)]\left(\frac{12.5(n-2)}{1-(n-2)}\right)^{n-2} \quad \ldots (6)$$

Figure 11 displaysa plot of load P against yield strength, wherein an enhancement in the graph of doped sample is observed.The elastic stiffness constant ($C_{11}$) was calculated using the formula[22] Wooster empirical relation,

$$C_{11} = H_v^{7/4} \quad \ldots (7)$$

The value of $C_{11}$ is determined by two crucial elements. The first factor is how tightly the atoms are

bonded to one another. The second factor is the rate at which the forces of attraction and repulsion between atoms vary with their positions[23]. The plots of stiffness constant vs Load P of Pure & Crystal Violet doped LAM are displayed below (Figs.12 -13).

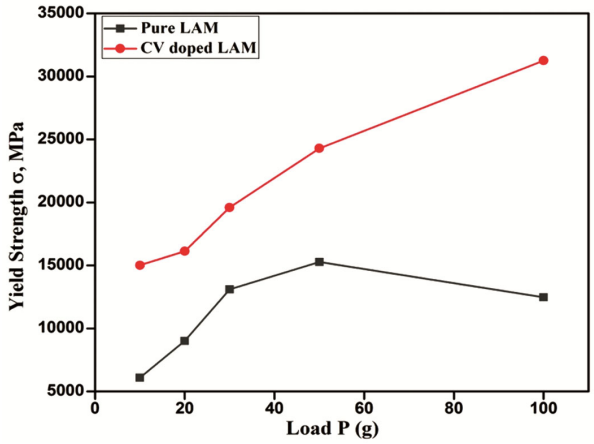


Fig. 11 — Plot of σ vs Load P of Pure CV doped LAM crystals

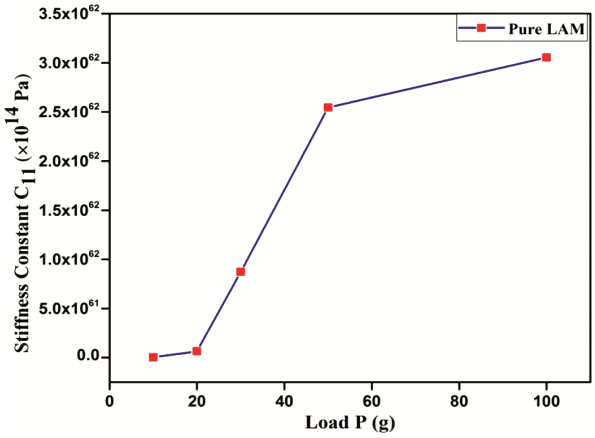


Fig. 12 — $C_{11}$ vs Load P of Pure LAM crystal

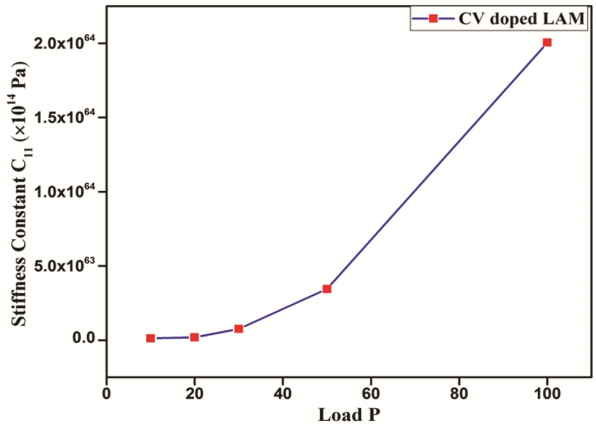


Fig. 13 — $C_{11}$ vs Load P of CV doped LAM crystal

### 3.5 Thermal Evaluation

The TG/DTA analysis is a powerful technique used to analyze crystals and other materials by measuring mass changes and heat flow under controlled temperatures[24]. TGA measures the change in mass of the crystal sample and DTA measures the change in heat flow at various temperatures.In the nitrogen environment, Figs. 14-15 displays the TG/DTA curves of pure and crystal violet dye doped LAM crystal samples by a heating rate of 10 °C min−1, between 40 and 500 °C temperature range. For Pure LAM crystal sample,it is evident that the formed crystal was found to be thermally stable up until 205°C and that there is no phase change or weight loss between 40 and 205°C. Distinct endothermic peak at 198°C in pure crystal indicates dehydration where heat is absorbed and therefore water molecules are removed and it is also called the decomposition point of the sample. For CV doped LAM crystal, there occurs two phase transitions, one occurring at 112°C might be the result of a shift in crystal structure and the second phase transition occurring at 190°C could most likely be due to decomposition of the crystal.

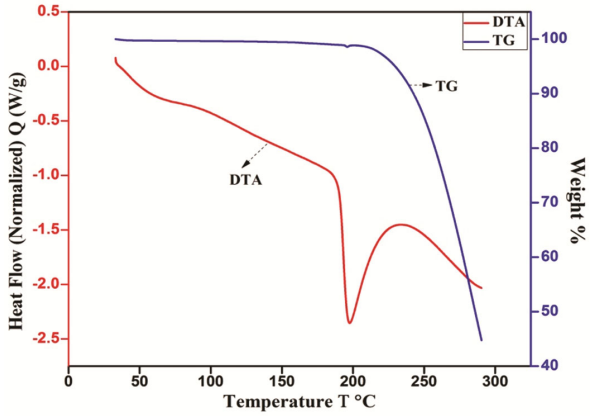


Fig. 14 — TG/DTA curve of Pure sample

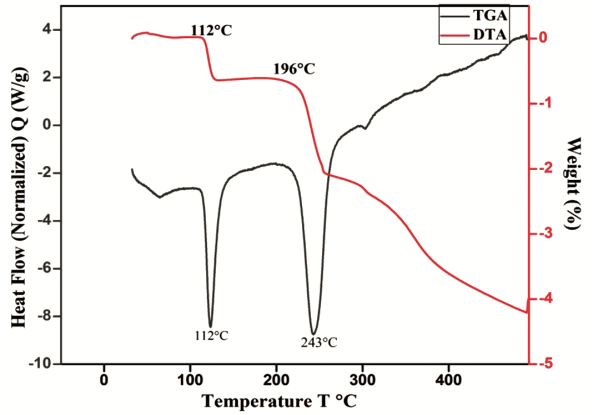


Fig. 15 — TG/DTA curve of doped sample

The first endothermic peak occurring at 123°C generally indicates a phase transition or decomposition event that absorbs heat. An endothermic peak corresponding to 243°C indicates dehydration where heat is absorbed and therefore water molecules are removed andIt is also known as the decomposition point or the sample's breakdown point.Good crystallinity was suggested by the sharp endothermic peak at 243°C, which also verifies that the materials are free of residue and contaminants.

**3.6 Antibacterial Activity**

The crystal's antimicrobial activity was examined to look into its potential biological uses. The antimicrobial properties of the compounds,The technique of agar well diffusion was employed to examine pure LAM and Crystal Violet doped LAM crystal samples against gram negative bacteria, such as Klebsiella pneumonia and pseudomonas aeruginosa, and gram positive bacteria, such as Staphylococcus aureus and Streptococcus mutans. Table 2 - 3 depicts the antibacterial of both Pure & CV doped LAM crystals.

For Pure LAM crystal, it exhibits 20 mm of activity against Saureus, an excellent activity of 22 mm against Smutans, 24 mm of activity against Paeruginosa, and an activity of 20 mm against Kpneumonia.The sample under inquiry is active against the bacteria if the inhibition zone has a diameter greater than 7 mm.Conductivity, solubility, and intermolecular interactions could be the causes of the activity[25, 26]. For CV doped LAM crystal, it exhibits 18 mm of activity against S aureus, an excellent activity of 22 mm againstS mutans, 18 mm of activity against P aeruginosa, and an activity of 18 mm against K pneumonia. Pure and CV doped crystals can be widely employed in biomedical and water purification applications due to its antibacterial properties. The photographs of inhibition zones for four different bacteria for pure & dye doped samples are displayed below (Figs. 16-17).

Table 2 — Zone of inhibition for Pure LAM crystal

| Bacterium | Zone of inhibition (mm) | |
|---|---|---|
| | Pure LAM | Standard (Chloramphenicol) |
| Streptococcus aureus | 20 | 18 |
| Streptococcus mutans | 22 | 15 |
| Pseudomonas aeruginosa | 24 | 30 |
| Klebsiella pneumonia | 20 | 20 |

Table 3 — Zone of inhibition for CV doped LAM crystal

| Bacterium | Zone of inhibition (mm) | |
|---|---|---|
| | CV doped LAM | Standard (Chloramphenicol) |
| Streptococcus aureus | 18 | 18 |
| Streptococcus mutans | 22 | 15 |
| Pseudomonas aeruginosa | 18 | 30 |
| Klebsiella pneumonia | 18 | 16 |

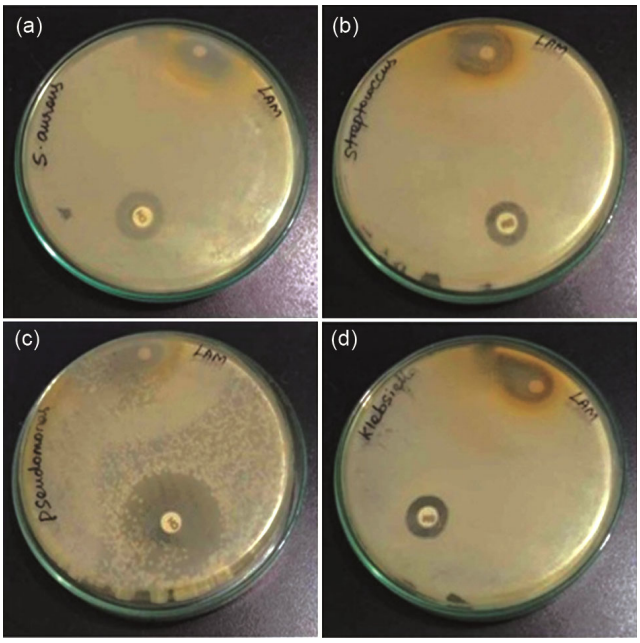


Fig. 16 — Inhibition zones of Pure LAM against a) S aureus, b) S mutans, c) P aeruginosa and d) K pneumonia

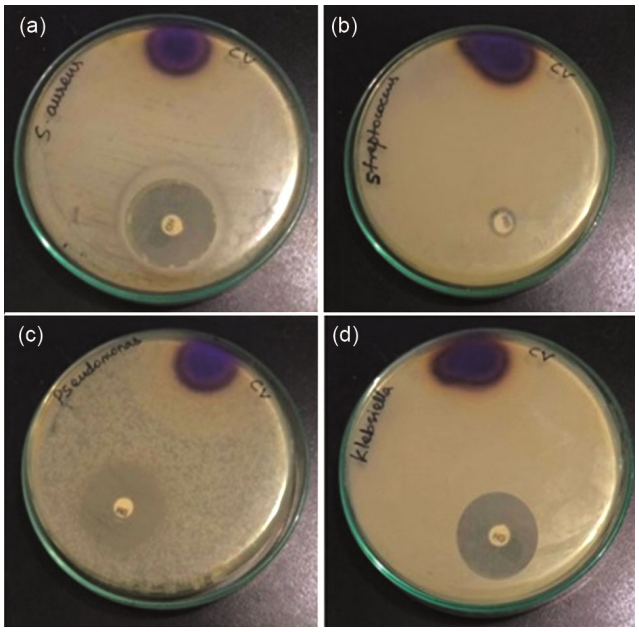


Fig. 17 − Inhibition zones of CV doped LAM against a) S aureus ,b) S mutans, c) P aeruginosa and d) K pneumonia

## 4 Conclusion

To change the characteristics of L-asparagine crystal, crystal violet has been incorporated into its lattice. The slow evaporation solution growth method was used to cultivate the single crystals of crystal violet doped L-asparagine. It was then discovered that its structure was modified and that the developed Crystal Violet doped LAM crystal has a triclinic crystal structure. Doping crystal violet into L-asparagine crystal has been shown to alter the crystal structure. Powder XRD showed that the Pure LAM crystal has orthorhombic crystal structure and CV doped LAM crystal has triclinic crystal structure. The transmittance spectra of undoped and CV-doped L-asparagine crystals showed fundamental cutoff wavelengths of 260 nm and 246 nm, respectively. It was discovered that the Crystal Violet doped crystal's energy band gap value was marginally larger than the undoped L-asparagine crystal. The mechanical characteristics of pure and crystal violet doped L-asparagine single crystals, such as its hardness against strain,its yield strength, and the material's stiffness constant, have been identified. Using Thermal Analysis technique, a good thermal stability up until 205 °C for Pure LAM sample and 112°C for CV doped LAM was obtained. Four strains of Pseudomonas aeruginosa, Klebsiella pneumonia, Streptococcus mutans, and Staphylococcus aureus were used to investigate the antibacterial activity using the Agar disk diffusion test. The sample was shown to have the highest activity against Streptococcus mutans at 22 mm. Consequently, the generated samples were shown to have a wide range of applications in the domains of electro-optics, water purification, and biomedicine.

## Acknowledgement

The writers express their gratitude to the Manonmaniam Sundaranar University, Tirunelveli, and Kalasalingam University, Rajapalayam, and The M.D.T Hindu College, Palayamkottai, and Smykon Biotech Pvt Ltd, Nagercoil for their support in data analysis.

## References

1 Moody G & Islam MS, *MRS Bulletin,* 47 (2022) 475.
2 Amsalu K & Palani S, *Mater Today Proc,* 33 (2020) 3372.
3 Wen S, Wang T, Zhang X, Hu X & Wu Y, *J Environ Chem Eng,* 12 (2024) 112533.
4 Alka G & Ritu D, *Indian J Pure Appl Phys,* 61 (2023) 998.
5 Krall A, Xu S, Graeber T, Daniel Braas D & Christofk HR, *Nat Commun,* 7 (2016) 11457.
6 Gracelin Juliana S, Sathishkumar P & Vella Durai S C, *Indian J Pure Appl Phy,* 62 (2024) 1098.
7 Bharagava R N, Mani S, Mulla SI & Saratale GD, *Ecotoxicol Environ Saf*, 156 (2018) 166.
8 Dey S & Nagababu B H, *Food Chem Adv*, 1 (2022) 100019.
9 Arul Tresa M, Helina B & Vella Durai S C, *Indian J Pure Appl Phys*, 62 (2024) 631.
10 Caroline O, Roger J D, Cruz-Cabeza A J & Vetter T, *Cryst Growth Des*, 25 (2025) 1644.
11 Cameron F H & Raymond ES, *ACS Nano*, 13 (2019) 7359.
12 Dhiman P, Rana G, Kumar A, Dawi E A & Sharma G, *Molecules*, 28 (2023) 2838.
13 Bellefqih H, Bilal E, Fakhreddine R, Mehdaoui B, Haneklaus N & Aatiq A, *Inorg Chem Commun*, 163 (2024) 112347.
14 Goel S, Sinha N, Yadav H, Joseph AJ, Hussain A & Kumar B, *Arabian J Chem*, 13 (2020) 146.
15 Manuel AP & Shankar K, *Nanomaterials,* 11 (2021) 1249.
16 Mia M N H, Pervez M F, Khalid Hossain M, Reefaz Rahman M, Jalal Uddin M, Al Mashud M A, Ghosh H K & Mahbubul H, *Results Phys*, 7 (2017) 2683.
17 Saini R & Joseph D, *Mater Today Proc*, (2024).
18 Sinha N, Batra K, Bhukkal S, Kumar R, Kumar S, Goel S & Kumar B, *Arabian J Chem*, 13 (2020) 5750.
19 Mancuso A, Blangetti N, Sacco O, Freyria F S, Bonelli B, Esposito S, Sannino D & Vaiano V, *Nanomaterials*, 13 (2023) 270.
20 Shukla M, Sinha N, Sagar P, Yadav T, Kumar R & Kumar B, *Spectrochim Acta A*, 321 (2024) 124722.
21 Ozturk O, Safran S, Ada H, Bulut F, Seydioglu T, Nefrow A R A, Akkurt B, Terzioglu C & Yildirim G, *J Mater Sci Mater Electron,* 35 (2024) 1018.
22 Boopathi K & Ramasamy P, *Spectrochim Acta A*, 126 (2014) 7.
23 Agmo Hernández V, *Chem Texts,* 9 (2023) 10.
24 Sherine S S, *Biomat J*, 2 (2023) 13.
25 Zhang Q K, Yue CP, Zhang Y & Liu Z Y, *Inorg Chim Acta*, 473 (2018) 112.
26 Gautam B, Dani R, Prasad R, Srivastava M, Yadav R & Gondwal M, *Pharm Cta*, 6 (2015) 1.